



DEPARTMENT OF MECHANICAL ENGINEERING
INDIAN INSTITUTE OF INFORMATION
TECHNOLOGY, DESIGN AND
MANUFACTURING KANCHEEPURAM
CHENNAI - 600127

Synopsis Of

**DEVELOPMENT OF BUILD
STRATEGIES FOR THIN-WALLED
Ti6Al4V COMPONENTS USING LASER
POWDER BED FUSION PROCESS**

A Thesis

To be submitted by

S JAGATHEESHKUMAR

For the award of the degree

Of

DOCTOR OF PHILOSOPHY

1 Abstract

Complex thin-walled components find numerous applications in aerospace, automotive and marine domains to meet the demands in design, manufacturing, durability, reliability, fuel efficiency and sustainability due to their superior properties. Although thin-walled components offer several advantages, their manufacturing presents significant challenges, especially when it comes to achieving the required geometric characteristics, uniform distribution of tolerances, surface integrity, consistency and accuracy. Laser Powder Bed Fusion (LPBF) has created interest for the industries, in particular, aerospace sectors to produce metallic components with complex geometries directly from the CAD model. In the LPBF process, a thin layer of material is selectively melted and solidified, resulting in the creation of a dense and precise geometric structure. However, the high temperature gradient developed in this process due to the rapid heating and cooling cycles leads to thermal distortions which cause dimensional inaccuracies and significant variation in the mechanical performance of the parts. Therefore, the present work is focused on the development of a systematic approach based on the inherent strain method, viz. Ansys Additive Print (AAP) software to predict the residual stresses and thermal distortion induced in thin-walled Ti6Al4V components and to improve the quality of parts produced in LPBF. During the development of the work, a single cantilever beam was initially considered. Subsequently, the study was extended to the aero-engine compressor, as these components are a suitable representation of thin-walled parts. The process parameters, such as laser power, scan speed, and hatch distance, were varied extensively in this study. It can be noted that 20.4% deviation in residual stress and 5% deviation in maximum distortion were seen between numerical predictions and the experimental measurements. Additionally, it was found that the lower energy density resulted in a significant reduction in residual stress and thermal distortion in the selected components.

Microstructure and mechanical property are significantly affected by the input process parameters, therefore, the study was extended further on this investigation. Ti6Al4V specimens were fabricated using EOS M280 machine, considering three different energy densities as similar to the residual stress and distortion study. Increase in energy density may result in increase in width (129 μm to 165 μm) of the prior β -grain boundaries. No significant change in yield strength was observed in specimens built with lower energy densities. Furthermore, thin-walled components will experience extreme dynamic loading conditions during its service operations. Due to this, the material will undergo severe large deformations. Hence, the study was conducted to assess the dynamic compression behaviour of Ti6Al4V alloys at high strain rates using Split-Hopkinson Pressure Bar (SHPB) experiments. SHPB tests were performed for the varying strain rates ranging from 1100 s^{-1} - 3300 s^{-1} . LPBF-built samples exhibited high strain rate sensitivity, $m > 0$ under dynamic compression, which means that the flow stress increases as the strain rate increases. It was also observed that there is no significant change in yield strength for samples built with low energy density. At low energy density, the formation of a hierarchical structure of relatively fine α' -martensite, separated from each other by a high dislocation density, leads to increase in yield strength. Dynamic compression of as-built and heat treated samples were compared and found

that heat treated samples exhibited 12% lower yield strength than the as-built samples, as expected; this yield strength reduction is due to the transformation of α' martensite to α , lamellar $\alpha + \beta$ and retained β as confirmed by microstructure and SEM studies. Based on the above findings, it can be concluded that the usage of low energy density in LPBF process exhibits superior yield strength with significant reduction in residual stress and thermal distortions in the thin-walled Ti6Al4V components.

2 Research gap and the objectives

In LPBF process, particularly during the manufacturing of thin-walled parts, a high residual stresses and distortions are induced due to high thermal gradients involved in the process as reported in recent studies (Bartlett and Li (2019)). The high residual stresses and distortions lead to part failures and affect the mechanical properties of the built components (Parry *et al.* (2016)). The successful realization of Ti6Al4V components using LPBF technique requires consideration of multiple factors, including laser powder interaction, melt pool dynamics, thermal gradients and phase transformations during the process. It was observed from the published literature that the selection of input process parameters are very crucial for the LPBF process, especially for the fabrication of Ti6Al4V thin-walled components. Many researchers have attempted to understand the relationship between input process parameters and the residual stress, as well as thermal distortions developed in LPBF built parts using numerical simulation such as thermo-mechanical analysis or an inherent strain approach with experimental validations Wu *et al.* (2017); Bompos *et al.* (2020); Chen *et al.* (2019)). The high-fidelity thermo-mechanical modelling approach currently faces challenges in the analysis of complex industrial-size components due to the requirement of extensive computational resources and time. Despite the tremendous progress in LPBF simulation, the inherent strain method is more efficient and cost-effective for analysing complex parts with reasonable accuracy. Most researchers have validated the numerical predictions by comparing the experimental measurements. The calibration of inherent strain is an important step in this analysis which determines the accuracy of numerical predictions; however, no clear guideline is available to extract the inherent strain values and to predict the residual stress and distortion, specifically for the complex thin-walled structures such as aero-engine compressor blade, turbine blade and rotor components.

In addition, most of the studies were conducted to optimize the process parameters for minimizing residual stresses and distortion in the material without considering its microstructure changes and the mechanical characteristics. The microstructure of Ti6Al4V alloy is very sensitive to the thermal history and is susceptible to inherent phase transformations during the LPBF process, and the resultant mechanical properties are mainly depends on the micro structural behaviour of printed components (Sun *et al.* (2019); Ali *et al.* (2018)). Also, the aero-engine parts may undergo severe large deformation due to its service life operations and the nonlinearity of the materials, but a limited number of studies were done on the effect of material behaviour at high strain rates. Therefore, the present research is focused on the development of a systematic numerical simulation framework using inherent strain method to study the effect of process parameters on residual stress and distortions in the thin-walled Ti6Al4V components and to investi-

gate the influence on microstructure and mechanical behaviour under quasi-static and high strain rate conditions, specifically suitable for the manufacturing of thin-walled aero-engine components.

The following objectives are arrived to fulfil the above research gaps.

- (i) To develop a systematic numerical simulation strategy for predicting the residual stress and distortion in the Ti6Al4V-based LPBF built thin-walled components, with consideration of most influencing input process parameters such as laser power, scanning speed, hatch distance and layer thickness;
- (ii) To perform experimental measurements of residual stress and thermal distortions in the LPBF built specimens.
- (iii) To understand the microstructure behaviour of the LPBF built parts that are manufactured using the optimized process parameters;
- (iv) To understand the mechanical properties of the LPBF built specimens that are fabricated using the process parameters optimized in objective 1.
- (v) Finally, to deploy a validated numerical simulation guideline along with the suitable process parameters for manufacturing of thin-walled Ti6Al4V aero-engine components such as compressor blades.

3 Methodology

The methodology adopted for the present study is given as a flow chart in Figure 1.11 to illustrate the various steps to meet the research objectives.

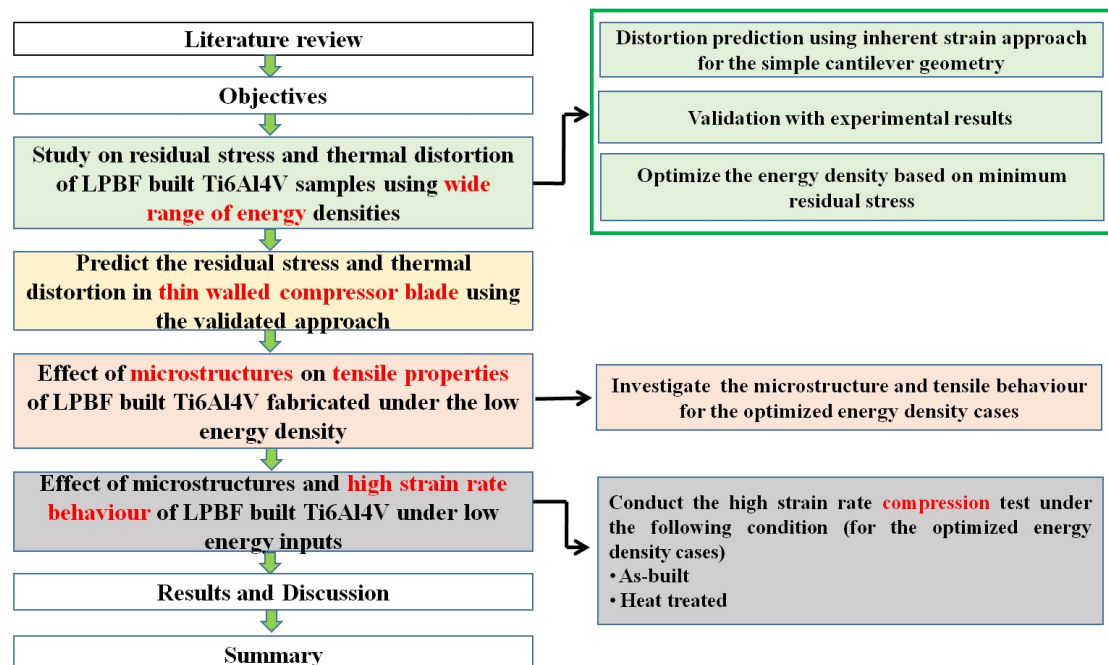


Figure 1: Work flow diagram

4 Most Important Contributions

4.1 Numerical frame work to predict the residual stress and distortions

In Chapter 2, a systematic guideline using Ansys Additive Print (AAP) software has been developed for predicting the residual stress and thermal distortions in the single cantilever specimens made of aerospace grade Ti6Al4V alloy. AAP uses inherent strain approach and the calibration of inherent strain coefficient is the key parameter to predict the residual stress and distortion in the part level. A step by step procedure for the calibration of inherent strain coefficients have been developed with an aid of numerical simulation and experimental building of test coupons. The calibrated inherent strain coefficient values were used for the prediction of residual stresses and distortions in the thin-walled representative geometry viz. single cantilever beam. The laser power (P), scan speed (v_s) and hatch distance (h) were found to be most influencing parameters and these parameters varied (as a function of energy density as given in Eq. (1)) from $E_v = 27.78 \text{ J/mm}^3$ to $E_v = 79.17 \text{ J/mm}^3$ within the LPBF Ti6Al4V v_s space Promoppatum *et al.* (2017), whereas as a constant layer thickness (t) of $30 \mu\text{m}$ have been considered in the present work.

$$E_v = \frac{P}{v \times h \times t} \quad (1)$$

The residual stress and distortion values at different locations of the cantilever specimen were predicted using numerical simulation for the wide range of energy density. In order to validate the numerical predictions, the cantilever specimens were fabricated using EOS INT M280 machine for the selected energy density cases ($E_v=36.27 \text{ J/mm}^3$, 45.33 J/mm^3 and 75.56 J/mm^3) and the residual stresses and distortion were measured experimentally using XRD and 3D optical scanner.

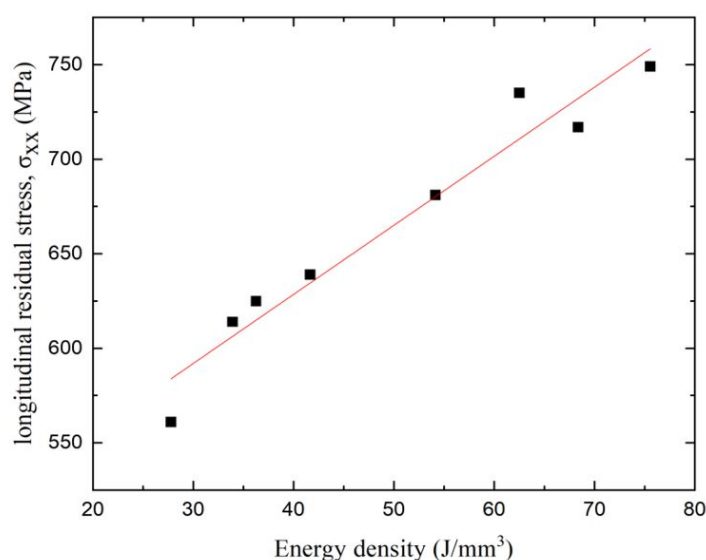


Figure 2: Effect of energy density on residual stress with in calibrated region

The numerically predicted residual stress and distortion were found to be matching well with the experimental measurement values. The effect of energy density on residual stress and distortion was studied using AAP and it was noted that the lowering of energy density helps to reduce residual stress and distortion in the part with in the calibrated region as shown in Figure 2.

4.2 Residual stress and distortion in thin walled aero engine compressor blade

In Chapter 3, the developed numerical framework using AAP (section 4.1) has been adopted to predict the residual stress and distortion in the aircraft engine compressor blade. Three different energy densities in the low energy density range of the safe operating window (P - vs space) were selected such as (i) Case 1: $E_v = 41.67 \text{ J/mm}^3$, (ii) Case 2: $E_v = 45.33 \text{ J/mm}^3$ and (iii) Case 3: $E_v = 52.78 \text{ J/mm}^3$. The inherent strain coefficient was calibrated for the above selected energy density cases using the cross-walled geometry, which is a representative geometry for thin-walled structures. The calibrated inherent strain coefficients were used to simulate the compressor blades to predict the residual stresses and thermal distortions. In addition, the compressor blade was manufactured using the EOS INT M280 machine considering the manufacturing conditions defined in the numerical simulation. The residual stress and distortion were measured using experimental means, utilizing an XRD and 3D optical scanner respectively.

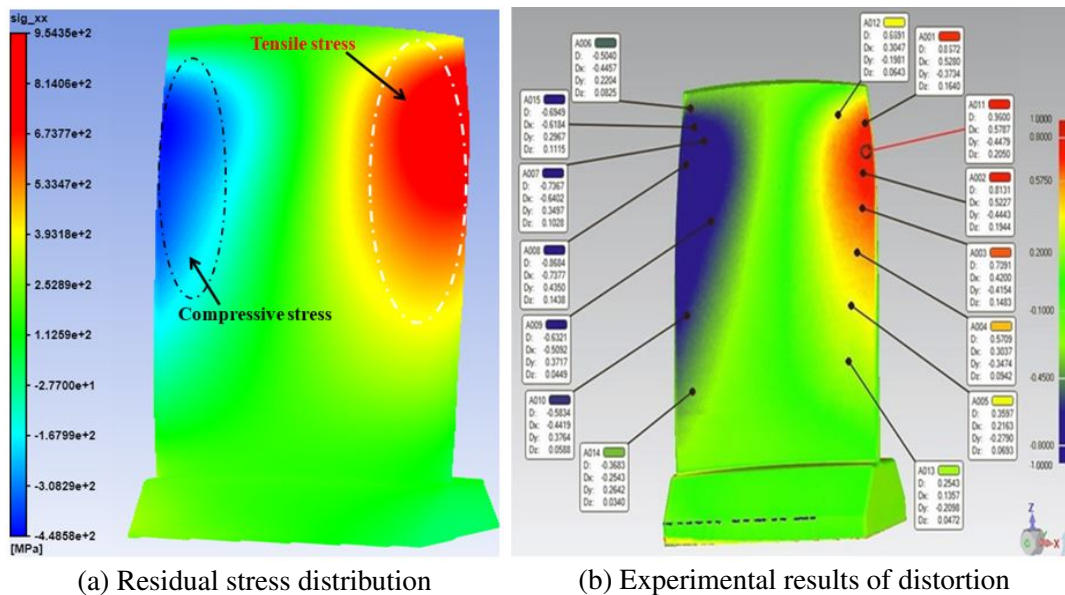


Figure 3: Comparison of numerically predicted residual stress and experimental distortion of compressor blade

The numerical prediction of residual stresses was found to be matching well (20 % deviation) with the corresponding experimental results within the calibrated regime. The maximum residual stress is developed on the leading and trailing edges of the blade for all the energy density cases considered. The residual stress value increases as the build height progress. The distortion distribution is consistent with residual stress distribution

as shown in Figure 3 and the maximum value of distortion occurs, where the residual stress values are high. Minimizing the thermal gradients and cooling rates, which have a greater impact on thin-walled sections than the thicker parts. Therefore, the careful selection of process parameters including laser power, hatch spacing, scanning speed, layer thickness and scanning strategy is found to be useful to control the residual stress and the thermal distortion in the thin-walled components.

4.3 Quasi-static tensile and microstructure behaviour

Residual stresses and thermal distortions are always present in the manufactured parts using LPBF process due to high thermal gradients and rapid changes in heating and cooling rates, which cannot be completely eliminated. Several researchers have attempted to minimize the residual stresses and distortions in the LPBF-built components by controlling its input process parameters. However, the microstructure and mechanical properties of the components manufactured in LPBF are very sensitive to the thermal history, especially, the Ti6Al4V-dual phase alloy, which means that there is a direct relationship between the input process parameters and the microstructure as well as the mechanical behaviour of the built parts. Microstructure and mechanical properties of the as-built LPBF components are highly anisotropic and exhibit poor ductility due to the existence of a α' -near full martensitic phase; hence, these properties are significantly different from the conventionally processed Ti6Al4V parts. Therefore, the effect of process parameters on microstructure analysis and the mechanical property characterization of Ti6Al4V alloy was carried in Chapter 4. The tensile specimens (three specimens in each process parameter set) were fabricated to determine the tensile properties for three different energy densities as investigated in section 4.2 for the aero-engine compressor blades. Fractography and microstructural analysis were performed to understand the influence of input parameters on the internal grain structure, as it directly affects the mechanical behaviour of the material. The study reveals that, the increase in energy density from 41.67 J/mm^3 to 52.78 J/mm^3 may result in an increase in width ($129 \mu\text{m}$ to $165 \mu\text{m}$) of the prior β -grain boundaries; A typical hierarchical structure of acicular α' martensite found within the coarse prior β grains. Furthermore, the self-accommodation of α' during rapid cooling makes the α' -needles to incline at specific orientation to each other Huang *et al.* (2015). This accommodation follows Burger's Orientation Relationships (BOR) between the β and α/α' a given in Eq. (2) Vrancken *et al.* (2012).

$$\{110\}\beta \parallel \{0001\}\alpha \text{ and } \langle 111 \rangle \beta \parallel \langle 1120 \rangle \alpha \quad (2)$$

No significant change in ultimate tensile strength was observed in specimens built with energy densities of 41.67 J/mm^3 and 45.33 J/mm^3 as shown in Figure 4. However, the samples prepared with low energy density exhibit higher tensile strength than samples with high energy density due to the formation hierarchical structure of fine α' martensite laths. A cleavage facet with dimple networks in the fracture surface indicates that the sample exhibits the combination of brittle and ductile failure mechanism of the as-built LPBF samples. A shallow dimple becomes deeper and larger with increasing energy density, which improves ductility. Based on the findings from microstructure and tensile behavior, it is obvious that the usage of low energy density in LPBF process yields highest tensile strength of the Ti6Al4V aero-engine components.

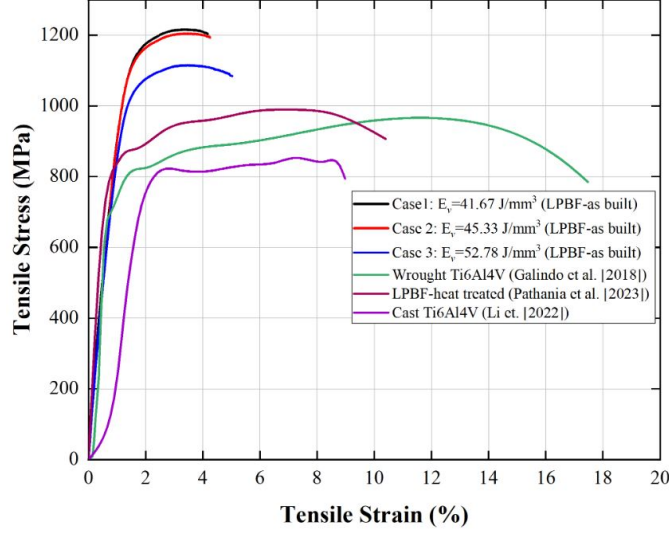


Figure 4: Comparison of tensile stress - strain behavior under different conditions Galindo-Fernández *et al.* (2018); Pathania *et al.* (2023); Li *et al.* (2022)

4.4 High strain rate compression behaviour

Thin-walled aero-engine compressor components will experience extreme dynamic loading conditions during its service operations. Due to this, the material will undergo severe large deformations. Hence, the study was conducted to understand the dynamic behaviour of Ti6Al4V alloys at high strain rates using Split-Hopkinson Pressure Bar (SHPB) experiments were detailed in Chapter 5. The cylindrical samples were built using EOS INT 280 machine and machined using wire EDM of 6 mm diameter with 4 mm height. The SHPB tests were conducted at varying strain rates (1178 s^{-1} , 2170 s^{-1} and 3260 s^{-1}) to investigate the dynamic compression behavior of LPBF Ti6Al4V alloy built using the lower energy density case 1: $E_v = 41.67 \text{ J/mm}^3$. And the effect of energy density on the dynamic compressive behaviour of LPBF built Ti6Al4V alloy was explored for samples built with different energy densities, such as (i) case 1: $E_v = 41.67 \text{ J/mm}^3$, (ii) case 2: $E_v = 45.33 \text{ J/mm}^3$, and (iii) case 3: $E_v = 52.78 \text{ J/mm}^3$ which are similar to the study conducted for the compressor blade and microstructure and mechanical behaviour (refer section 4.2 and 4.3). Further the dynamic compression behavior of as-built samples (case 1: $E_v = 41.67 \text{ J/mm}^3$) were compared with heat treated samples to account the effect of heat treatment. The SHPB experiments were performed for the varying strain rates ranging from 1100 s^{-1} - 3300 s^{-1} . The general parameter that quantifies the material behaviour at different strain rates is the strain rate sensitivity, which is denoted by m in Eq. (3) Alkhatib and Sercombe (2022).

$$m = \left(\frac{\partial \ln \sigma}{\partial \ln \dot{\epsilon}} \right) = \frac{\ln \left(\frac{\sigma_2}{\sigma_1} \right)}{\ln \left(\frac{\dot{\epsilon}_2}{\dot{\epsilon}_1} \right)} \quad (3)$$

where, σ_2 and σ_1 are the true stress values at a certain strain, at strain rates $\dot{\epsilon}_1$ and $\dot{\epsilon}_2$ respectively.

LPBF-built samples exhibited high strain rate sensitivity, $m > 0$ under dynamic compression, which means that the flow stress increases as the strain rate increases. It was also observed that there is no significant change in yield strength for samples built with energy density of Case 1: $E_v = 41.67 \text{ J/mm}^3$ and Case 2: $E_v = 45.33 \text{ J/mm}^3$ as shown in Figure 5a. At lower energy density case, the formation of a hierarchical structure of relatively fine α' martensite, separated from each other by a high dislocation density, which effectively hinders the movement of dislocations during deformation and leads to higher strength. Additionally, dynamic compression of as-built and heat treated samples were compared and found that heat treated samples exhibited 12% lower yield strength than the as-built samples (see Figure 5b), as expected; this yield strength reduction is due to the transformation of α' martensite to α , lamellar $\alpha + \beta$ and retained β as confirmed by microstructure and SEM studies.

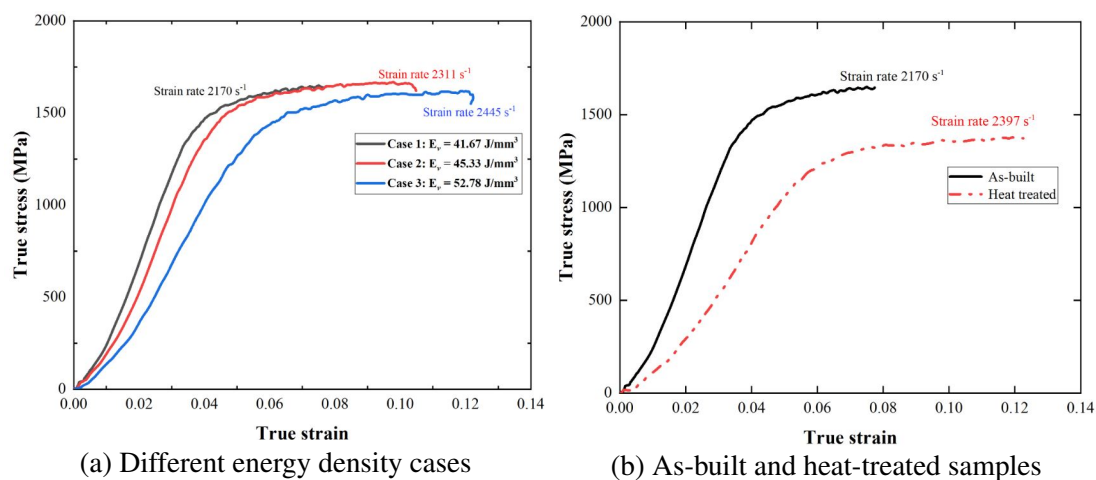


Figure 5: Dynamic responses of LPBF-built Ti6Al4V samples

5 Conclusions

The following conclusions can be drawn from the present research which are:

- (i) A systematic numerical simulation guideline has been developed for predicting the residual stress and thermal distortions using the single cantilever specimens. The numerically predicted results were compared with the experimental measurements and it was observed that the numerical results agreed with the experimental results up to a 20.4% deviation in residual stress and a 5% deviation in maximum distortion. Additionally, the effect of energy density ($E_v = 27.78 \text{ J/mm}^3$ to 79.17 J/mm^3) on residual stress and distortion was studied; lowering of energy density shows an significant reduction of residual stress and distortion in the parts.
- (ii) Guidelines developed for the single cantilever beam was adopted for predicting the residual stress and thermal distortions in the LPBF-built thin-walled aero-engine compressor blade component. Residual stresses were found to match with 20% deviation with the corresponding experimental results within the calibrated regime

and the distribution of distortion is almost identical to the experimental measurements. Therefore, the developed approach can be considered as a guideline for predicting and compensating the part distortion for the thin-walled Ti6Al4V based components in many engineering applications.

- (iii) From the microstructure and tensile behaviour study it was observed that the increase in energy density from 41.67 J/mm^3 to 52.78 J/mm^3 may result in increase in width ($129 \mu\text{m}$ to $165 \mu\text{m}$) of the prior β -grain boundaries. No significant change in ultimate tensile strength was observed in specimens built with energy densities of 41.67 J/mm^3 and 45.33 J/mm^3 . It is obvious that the usage of low energy density in LPBF process exhibits higher yield strength of the Ti6Al4V alloy used in the manufacturing of thin-walled aero-engine components.
- (iv) The dynamic compression results reveals that the LPBF built samples exhibited high strain rate sensitivity i.e. $m > 0$, which means that the flow stress increases as the strain rate increases. It was also observed that there is no significant change in yield strength was observed for samples built with energy density of Case 1: $E_v = 41.67 \text{ J/mm}^3$ and Case 2: $E_v = 45.33 \text{ J/mm}^3$. At lower energy density case, the formation of a hierarchical structure of relatively fine α' martensite, separated from each other by a high dislocation density leads to higher strength. Additionally, dynamic compression of as-built and heat treated samples were compared and found that heat treated samples exhibited 12% lower yield strength than the as-built samples, as expected; this yield strength reduction is due to the transformation of α' martensite to α , lamellar $\alpha + \beta$ and retained β as confirmed by microstructure and SEM studies.

6 Future work

In the present research work, a systematic approach has been developed for predicting the residual stresses and thermal distortions using ANSYS Additive Print. Additionally, an extensive study was conducted on the effects of LPBF process parameters on microstructure and mechanical behavior under both quasi-static and high strain rate conditions. However, there are few more aspects to be studied further to fulfil the needs of the aerospace industry in manufacturing of thin-walled components, which are discussed as follows:

- (i) The effect of pre-heating of the build plate, dwell time, scan strategy, varying layer thickness and support structure on residual stress and distortion need to be included in the developed simulation guideline for improving the fidelity and accuracy of predictions.
- (ii) Simplified Machine Learning (ML) techniques can be adopted for reducing the computational time for analyzing the effect of process parameters on various aspects including residual stress, distortions, microstructure and mechanical properties.

7 Organization of the Thesis

The present thesis is organised into seven chapters and the summary of each chapter is given here:

Chapter 1 : Introduction

Chapter 2 : Numerical study of a single cantilever beam

Chapter 3 : Numerical study of a aero-engine compressor blade

Chapter 4 : Study of microstructure and mechanical behaviour

Chapter 5 : Study of High strain rate behaviour

Chapter 6 : Conclusions and future work

8 List of Publications

Journal

1. Jagatheeshkumar S, Raguraman M, Siva Prasad AVS, Nagesha B K, Chandrasekhar U, “Study of residual stresses and distortions from the Ti6Al4V based thin walled geometries built using LPBF process”, Def. Technol. 1–9 (2023).
<https://doi.org/10.1016/j.dt.2023.01.002>.
2. Jagatheeshkumar S, Raguraman M, Siva Prasad AVS, Nagesha B K, Chandrasekhar U “simulation driven methodology for distortion prediction in thin-walled compressor blade built using LPBF process”, Int. J. Interact. Des. Manuf., (2023).
<https://doi.org/10.1007/s12008-023-01560-w>.
3. Jagatheeshkumar S, Raguraman M, Kesavan D, “Study of the effect of LPBF process parameters on distortion and mechanical properties of Ti6Al4V components”, Prog. Addit. Manuf. [under review]
4. Jagatheeshkumar S, Raguraman M, “Study on high strain rate dynamic compression behaviour of LPBF built Ti6Al4V alloy” Int.J. Crashworthiness [under preparation].

International conference

1. Jagatheeshkumar S, Raguraman M, “Study of residual stresses and distortions from the Ti6Al4V based thin walled geometries built using LPBF process”, International conference on Impact and plasticity (IMPLAST), organized by IIT Madras, 2022.
2. Jagatheeshkumar S, Raguraman M, Kesavan D, “Mechanical and Microstructure Behaviour of Ti6Al4V Specimens Fabricated Using Laser Powder Bed Fusion”, 29th International conference on Processing and Fabrication of Advanced materials (PFAM), organized by IIT Tirupati, 2023.

References

1. **Ali, H., H. Ghadbeigi, and K. Mumtaz** (2018). Processing parameter effects on residual stress and mechanical properties of selective laser melted ti6al4v. *Journal of materials engineering and performance*, **27**, 4059–4068.
2. **Alkhatib, S. E. and T. B. Sercombe** (2022). High strain-rate response of additively manufactured light metal alloys. *Materials & Design*, **217**, 110664.
3. **Bartlett, J. L. and X. Li** (2019). An overview of residual stresses in metal powder bed fusion. *Additive Manufacturing*, **27**, 131–149.
4. **Bompos, D., J. Chaves-Jacob, and J.-M. Sprauel** (2020). Shape distortion prediction in complex 3d parts induced during the selective laser melting process. *CIRP Annals*, **69**(1), 517–520.
5. **Chen, Q., X. Liang, D. Hayduke, J. Liu, L. Cheng, J. Oskin, R. Whitmore, and A. C. To** (2019). An inherent strain based multiscale modeling framework for simulating part-scale residual deformation for direct metal laser sintering. *Additive Manufacturing*, **28**, 406–418.
6. **Galindo-Fernández, M., K. Mumtaz, P. Rivera-Díaz-del Castillo, E. Galindo-Nava, and H. Ghadbeigi** (2018). A microstructure sensitive model for deformation of ti-6al-4v describing cast-and-wrought and additive manufacturing morphologies. *Materials & Design*, **160**, 350–362.
7. **Huang, Q., X. Liu, X. Yang, R. Zhang, Z. Shen, and Q. Feng** (2015). Specific heat treatment of selective laser melted ti-6al-4v for biomedical applications. *Frontiers of Materials Science*, **9**, 373–381.
8. **Li, K., Y. Liu, X. Liu, X. Wu, S. Zhou, L. Zhang, W. Li, and W. Zhang** (2022). Simultaneous strength-ductility enhancement in as-cast ti6al4v alloy by trace ce. *Materials & Design*, **215**, 110491.
9. **Li, Y., K. Zhou, P. Tan, S. B. Tor, C. K. Chua, and K. F. Leong** (2018). Modeling temperature and residual stress fields in selective laser melting. *International Journal of Mechanical Sciences*, **136**, 24–35.
10. **Parry, L., I. Ashcroft, and R. D. Wildman** (2016). Understanding the effect of laser scan strategy on residual stress in selective laser melting through thermo-mechanical simulation. *Additive Manufacturing*, **12**, 1–15.
11. **Pathania, A., S. Anand Kumar, and B. Nagesha** (2023). Influence of post-heat treatment with super β transus temperature on the tensile behaviour of lpbf processed ti6al4v. *Proceedings of the Institution of Mechanical Engineers, Part E: Journal of Process Mechanical Engineering*, 09544089231209808.
12. **Promoppatum, P., R. Onler, and S.-C. Yao** (2017). Numerical and experimental investigations of micro and macro characteristics of direct metal laser sintered ti-6al-4v products. *Journal of Materials Processing Technology*, **240**, 262–273.
13. **Setien, I., M. Chiumenti, S. van der Veen, M. San Sebastian, F. Garciandía, and A. Echeverría** (2019). Empirical methodology to determine inherent strains in additive manufacturing. *Computers & Mathematics with Applications*, **78**(7), 2282–2295.

14. **Sun, D., D. Gu, K. Lin, J. Ma, W. Chen, J. Huang, X. Sun, and M. Chu** (2019). Selective laser melting of titanium parts: Influence of laser process parameters on macro-and microstructures and tensile property. *Powder technology*, **342**, 371–379.
15. **Vrancken, B., L. Thijs, J.-P. Kruth, and J. Van Humbeeck** (2012). Heat treatment of ti6al4v produced by selective laser melting: Microstructure and mechanical properties. *Journal of Alloys and Compounds*, **541**, 177–185.
16. **Wu, J., L. Wang, and X. An** (2017). Numerical analysis of residual stress evolution of als10mg manufactured by selective laser melting. *Optik*, **137**, 65–78.